ELSEVIER

Prediction of hERG potassium channel affinity by the CODESSA approach

Alessio Coi,[a,†] Ilaria Massarelli,[b,†] Laura Murgia,[b] Marilena Saraceno,[a]
Vincenzo Calderone[c] and Anna Maria Bianucci[a,*]

[a]*Dipartimento di Scienze Farmaceutiche, Università di Pisa, Via Bonanno 6, 56126 Pisa, Italy*
[b]*Dipartimento di Chimica e Chimica Industriale, Università di Pisa, Via Risorgimento 35, 56126 Pisa, Italy*
[c]*Dipartimento di Psichiatria, Neurobiologia, Farmacologia e Biotecnologie, Università di Pisa, Via Bonanno 6, 56126 Pisa, Italy*

Abstract—The problem of predicting torsadogenic cardiotoxicity of drugs is afforded in this work. QSAR studies on a series of molecules, acting as hERG K$^+$ channel blockers, were carried out for this purpose by using the CODESSA program. Molecules belonging to the analyzed dataset are characterized by different therapeutic targets and by high molecular diversity. The predictive power of the obtained models was estimated by means of rigorous validation criteria implying the use of highly diagnostic statistical parameters on the test set, other than the training set. Validation results obtained for a *blind set*, disjoined from the whole dataset initially considered, confirmed the predictive potency of the models proposed here, so suggesting that they are worth to be considered as a valuable tool for practical applications in predicting the blockade of hERG K$^+$ channels.
© 2006 Elsevier Ltd. All rights reserved.

1. Introduction

The QT interval of the electrocardiogram (ECG) represents the duration of ventricular depolarization and subsequent repolarization, which starts at the beginning of the Q wave of the QRS complex and terminates where the T wave returns to isoelectric baseline. Usually, QT interval prolongation is due to a reduced outward potassium current, during phase 2 and 3 of the action potential.[1] This delay in repolarization is the primary pharmacological mechanism by which class III antiarrhythmic drugs exert their beneficial effect. Conversely, when QT prolongation is excessive, it can be pro-arrhythmic and can degenerate into *Torsade de Pointes* (TdP), a unique polymorphic form of ventricular tachycardia. TdP appears on the ECG as continuous twisting of the vector of the QRS complex around the isoelectric baseline. TdP is potentially fatal and therefore it is a highly undesirable pharmacological effect as far as non-antiarrhythmic drugs are concerned.

QT interval is usually transformed into a 'corrected' value known as the QTc interval. QTc interval is independent of the heart rate and it is referred to a standardized heart rate of 60 bpm. At present, it is not clear whether arrhythmia development is more closely related to an increase in the QT (absolute) or QTc (relative) interval. However, most of the drugs that cause TdP are able to increase both values.

In recent years, several drugs were shown to induce QT/QTc prolongation and TdP. For this reason, the development of new chemical entities (NCEs) requires preclinical and clinical investigations on QT/QTc prolongation and effects on cardiac repolarization. This statement is based on the observation that K$^+$ channels play a prominent role in the repolarization process. In particular, the delayed rectifier current in phases 2 and 3 of ECG depends on both rapid (IKr) and slow (IKs) K$^+$ channels.[2] Moreover, the studies of molecular genetics of Type-2 Long QT syndrome (LQTS2), a life-threatening genetically transmitted disease, pointed out that a mutation in the human Ether-a-gogo-related gene (hERG) was responsible for the syndrome. This gene was later found to represent the molecular basis of the cardiac repolarizing current IKr. The hERG protein forms the ion channel responsible for IKr.

At present, no three-dimensional structure or theoretical models of the entire channel are available.[3] Two papers describing partial models of the pore appeared recently in the literature.[4,5] These models account for some experimental observation, but they do not appear at this moment to be optimal for rapid screening of a large number of diverse molecules.

Many QSAR studies have been developed about the hERG channel blockade, all of them supplying valuable interpretation keys in terms of the proposed pharmacophores.[6–9] The main issue, in exploiting the QSAR models in this particular field, is that drugs capable of binding the hERG channel and of inducing QT prolongation belong to different pharmaceutical classes and are characterized by high molecular diversity.[10]

In the QSAR study presented here, the CODESSA program was used.[11] This tool is capable of learning from a *training set* the molecular characteristics responsible for hERG K^+ channel blocking properties, by the development of equations that quantitatively correlate chemical features and the target property ($\log IC_{50}$ of the hERG blockade).

Models obtained from this approach were submitted to rigorous validation analysis and finally used for the prediction of hERG blockade by drugs belonging to an external *blind set*.

2. Methods

2.1. Database collection

IC_{50} data of hERG inhibition were obtained from the literature. A paper of Bains et al. reporting IC_{50} values from HEK cells stably transformed with the hERG gene supplied the biological data for QSAR analysis (Table 1).[12] Other molecules available in the literature with known IC_{50} values from HEK cells were added to the dataset.[13–24] The IC_{50} is expressed as μM: when considering $IC_{50} = 1$ μM as threshold for evaluating the interaction between the compounds and the channel, values of $\log IC_{50} < 0$ represent molecules capable of blocking the hERG K^+ channel.

2.2. Molecular structure optimization

Since no structural information was available for most compounds of interest, the molecular models were constructed by using standard geometries (standard bond lengths and angle) within the Sybyl molecular modeling program.[25] A molecular mechanic (MM) approach was applied on the entire dataset, in order to obtain reasonable 3D arrangements after energy minimization. Whenever possible, molecular structures were optimized after alignment on a common template, as hypothesized in a previous work by us.[26] In this study, very simple structural features responsible for the interaction with the hERG K^+ channel were examined in order to suggest some minimal common requirements, which could explain the molecule toxicodynamic pattern. The template

Table 1. Analyzed Compounds and their average hERG $\log IC_{50}$ (μM) in HEK cells

Id	Compound	Log IC_{50} (μM)
1	4-Aminopyridine[15]	3.64
2	Ambasilide	0.56
3	Amiodarone[16]	−0.08
4	Amitriptyline	0.28
5	Artemisin	2.04
6	Astemizole	−2.24
7	Azimilide	−0.13
8	Benzoylecgonine	3.6
9	Berberine	1.82
10	Budipine[17]	−0.07
11	Caffeine	0.69
12	Carbamazepine[18]	2.4
13	Chlorbutanol[19]	3.64
14	Chlorpromazine	0.9
15	Chromanol-293B	0.82
16	Ciprofloxacin	2.98
17	Cisapride	−1.7
18	Clarithromycin[20]	1.66
19	Clofilium	−1.9
20	Clotrimazole	0.48
21	Cocaethylene	0.08
22	Cocaine	0.64
23	Desloratadine	0.65
24	Desmethylastemizole	−1.53
25	Dexfenfluramine[21]	2.73
26	Diltiazem	1.83
27	Dofetilide	−1.72
28	Dolasetron	0.77
29	Domperidone	−0.79
30	Dronedarone[22]	−0.50
31	Droperidol	−1.21
32	E-4031	−0.7
33	Ebastine	−1.6
34	Ecgogninemethylester	3.78
35	EGIS-7229	0.82
36	EMD-60263	0.82
37	EMD-60417	0.12
38	EMD-66398	−0.05
39	EMD-66430	0.05
40	Erythromycin	2.95
41	Fluvoxamine[23]	0.58
42	Gatifloxacin	1.75
43	Glibenclamide	1.87
44	Glimepiride	1.87
45	Glyceryl-nonivamide	−1
46	Granisetron	0.57
47	Grepafloxacin	1.82
48	H-345/52 (Adekalant)	−1.05
49	Imipramine	0.53
50	Isobutylmethylxanthine	1
51	Ketanserin	1.65
52	Ketoconazole	0.03
53	Levofloxacin	2.96
54	Loratadine	0.32
55	Losartan	0.89
56	LY-97241	−2.8
57	Methylecgonidine	2.23
58	Mibefradil	0.16
59	Misolastine	−0.55
60	MK-499	−2.57
61	Nicotine	−0.57
62	Nifedipine	2.79
63	Nifekalant[24]	−0.18
64	Norastemizole	−1.57
65	Norpropoxyphene	0.56

Table 1 (continued)

Id	Compound	Log IC$_{50}$ (μM)
66	Ondansetron	−0.09
67	Phenobarbital[18]	3.48
68	Phenytoin[18]	2.38
69	Pilsicainide[25]	1.31
70	Propoxyphene	0.44
71	Pyrilamine	0.39
72	Quinidine	−0.26
73	Risperidone	0
74	Sertindole	−1.37
75	Sildenafil	2
76	Sparfloxacin	−0.12
77	Tamoxifen	0.2
78	Terfenadine	−1.44
79	Terikalant	−1.16
80	Vesnarinone	0.17
81	WAY-123398	−0.69
82	Ziprasidone[26]	−0.82

consists of a hydrocarbon chain, three or four atoms long, serving as a spacer between a basic sterically hindered nitrogen atom, and a more variable moiety such as carbonyls, aliphatic amine groups, or aromatic nitrogen atoms. The main characteristic of this second moiety is reasonably related to its possibility of acting as hydrogen-bond acceptor.

The default force field available in the Sybyl package was exploited for energy minimization. It was carried out with the conjugate gradient minimization algorithm, untill root-mean-square (rms) deviation 0.01 kcal/mol Å was achieved.

2.3. Computational methods

A large number of molecular descriptors can be calculated by the CODESSA program on the basis of the geometrical and electronic features of the molecules. Structural attributes include topological connectivity indices and properties depending on the charge distribution in the molecule. CODESSA uses statistical structure–property correlation techniques for the analysis of experimental data in combination with the calculated molecular descriptors. Several strategies are available for the effective search of the best multi-parameter correlation in the large space of the natural descriptors. Finally, values of the molecular property of interest can be predicted by means of one or more multi-parameter correlation equation(s), obtained in the previous steps.

2.4. Statistical analysis for model validation

Validation is a crucial aspect of any QSAR modeling. Often, a high value of q^2 [average of leave-one-out (LOO) cross-validated correlation coefficient R^2] is considered a proof of the high predictive ability of the models. The lack of correlation between the high q^2 and the high predictive ability of a QSAR model has been previously established and subsequently confirmed by Golbraikh and Tropsha.[27–30] In particular, they showed

that a high value of q^2 appears to be the necessary but not the sufficient condition for the model to have a high predictive power. Moreover, the author emphasized the importance of rigorously validating the QSAR models on a *test set* disjoined from *training set* in order to establish their reliability.

A number of criteria on the *test set* for estimating the predictive ability of QSAR models were followed in this work, as derived from the study of Golbraikh and Tropsha. In general, a 'real' QSAR model may have a high predictive ability if it is close to the 'ideal' one. For the 'ideal' QSAR model, the regression line of actual against predicted activities will bisect the angle drawn by positive directions of the orthogonal axes. This may imply that the correlation coefficient between the actual and predicted activities of the 'real' QSAR model must be close to 1 and regression line through the origin should be characterized by a slope (k) close to 1.

However, these criteria do not ensure that a QSAR model possesses high predictive power: even though the correlation between the actual and predicted activities for the *test set* is characterized by high R^2 and k is close to 1, the prediction of property values for molecules belonging to a virtual library may fail. It happens when the regression line through the origin and its correlation coefficients R_0^2 are not close enough to the regression line and to its R^2, respectively. For this reason, a further condition for the QSAR model to have a high predictive ability has to be taken into account: R^2 and R_0^2 must have similar values and their closeness has to be checked through the ratio $(R^2 - R_0^2)/R^2$ which should be at least <0.1.

On the basis of what has been highlighted above, a predictive model is accurately validated whenever the following conditions are simultaneously satisfied. Condition on the *training set*: $q^2 > 0.5$. Conditions on the *test set*: (i) $R^2 > 0.6$; (ii) $(R^2 - R_o^2)/R^2 < 0.1$; (iii) $0.85 \leqslant k \leqslant 1.15$.
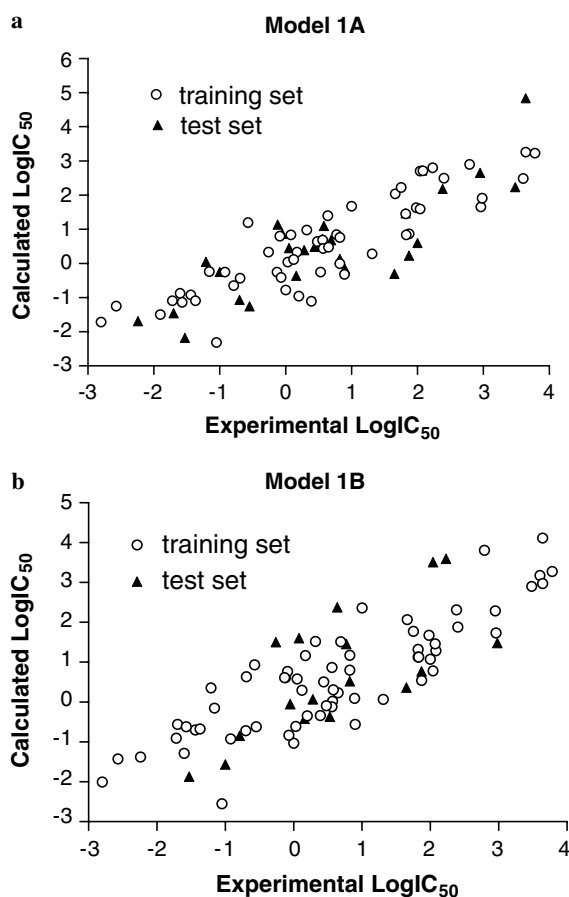
3. Results and discussion

3.1. CODESSA

The heuristic method, implemented in the CODESSA program for selecting the 'best' regression model, was applied to two different *training sets* chosen from the whole dataset made up of 82 molecules.[31]

The heuristic method for the descriptor selection proceeds with a pre-selection of descriptors by sequentially eliminating descriptors which do not match any of the following criteria: (a) Fisher F-criterion greater than 1; (b) R^2 value less than a value defined at the start (0.01); (c) Student's t-criterion less than that defined (0.1); and (d) duplicate descriptors having a higher squared inter-correlation coefficient than a predetermined threshold (usually 0.8), retaining the descriptor with higher R^2 referred to the property, in order to avoid redundant information. The remaining descriptors are

then listed in decreasing order of correlation coefficients when used in a global search for two-parameter correlations. Each significant two-parameter correlation by F-criterion is recursively expanded to an n-parameter correlation until the normalized F-criterion remains greater than the startup value. The top N-correlations by R^2 as well as F-criterion are saved.

The initial dataset was split into two *training* and *test sets*, in order to develop two different experiments labeled as 'A' and 'B'. The experiment 'A' was performed on *training* and *test sets* made up of 55 and 27 molecules, respectively; whereas the experiment 'B' was developed on *training* and *test sets* of 64 and 18 molecules, respectively.

Figure 1. Calculated versus experimental $\log IC_{50}$ for the *dataset* of 82 molecules in the twelve- (a) and in the nine-descriptor model (b).

The heuristic correlations performed for both 'A' and 'B' experiments provided some optimal equations with different number of descriptors ranging from 1 to 12. For the 'A' experiment, the best result are represented by a 12-parameter model with $R^2 = 0.77$ and $F = 11.85$. For the 'B' experiment the best result is represented by a nine-parameter model with $R^2 = 0.74$ and $F = 16.94$.

$\log IC_{50}$ values, calculated by both the twelve- and nine-parameter equations, for molecules belonging to the *training* and *test sets*, were plotted against the experimental values. Plots are reported in Figure 1a and b.

In spite of the different composition of *training sets* and of the different number of descriptors exploited in each experiment, five descriptors are shared by both models, thus meaning a good stability of the models themselves. QSAR equations for both models are reported in Table 2.

The most representative descriptors are the relative number of double bond (RNDB) and the factorized molecular volume (MV/XYZB) which negatively correlate to $\log IC_{50}$, leading to an increased blocking activity of the molecule.

The RNDB is the ratio between the number of double bonds divided by the total number of bonds and it is related to the rigidity and hydrophobicity of the molecule. The MV/XYZB is calculated as the ratio of the molecular volume and the volume of the parallelepiped box with the dimensions X_{max}, Y_{max}, and Z_{max} containing the molecule. It is related to the linearity (lack of globularity) of the molecule. Molecules characterized by a quite linear shape generally show high value of these descriptors.

On the contrary, the relative number of carbon atoms (RNCA is the ratio between the number of carbon atoms and the total number of atoms) and the relative negative charge (RNCG is the ratio between the maximum atomic negative charge and the overall negative charge in the molecule) positively correlate with the $\log IC_{50}$.
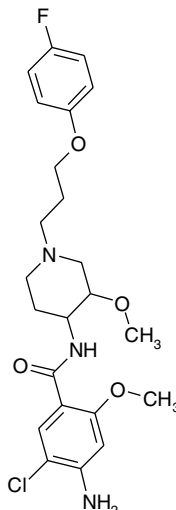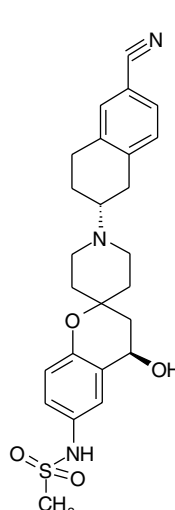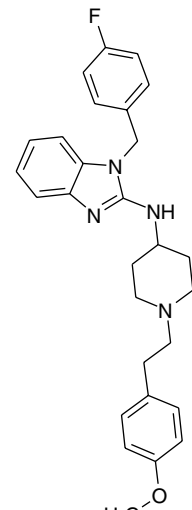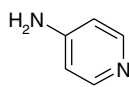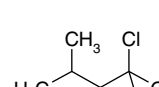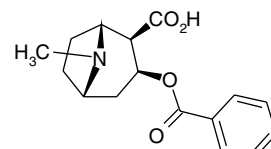
According to the CODESSA analysis, the contribution of RNDB and MV/XYZB descriptors highlights that hydrophobic features and size-related properties give rise to increased affinity to the hERG K^+ channel. These observations could explain the high ability to act as a blocking agent shown by large linear molecules present-

Table 2. QSAR equation for CODESSA models

Model	Equation
1A	$\log IC_{50} = -2.98 + 0.009\ PPSA1 + 0.5\ NOA - 2.6\ NTB + 4.1\ RPCG - 1\ KSI3 + 2\ BI + 0.03\ WNSA1 - 0.4\ RI3 - 20.5\ RNDB - 6.2\ ZXS/ZXR - 0.2\ NAB + 12.8\ RNCA$
1B	$\log IC_{50} = 1.6 + 0.01\ XYS + 0.6\ NOA - 2.5\ NTB + 9.9\ RPCG - 0.9\ KSI3 + 10.6\ RNCG - 10.5\ MV/XYZB - 0.4\ NR + 0.006\ WNSA-1$

PPSA1, partial positive surface area; NOA, number of oxygen atoms; NTB, number of triple bonds; RPCG, relative positive charge, KSI3, Kier shape index (order 3); BI, Balaban index; WNSA1, weighted negative surface area; RI3, Randic index (order 3); RNDB, relative number of double bonds; ZXS/ZXR, ZX shadow/ZX rectangle; NAB, number of aromatic bonds; RNCA, relative number of carbon atoms; MV/XYZB, molecular volume/XYZ box; NR, number of rings; XYS, XY shadow; RNCG, relative negative charge.

Table 3. Some 'blocking' and 'not-blocking' binders with their hERG $\log IC_{50}$ (µM) in HEK cells

Cisapride (-1.7)   MK-499 (-2.57)   Astemizole (-2.24)

4-amino-pyridine(3.64)   Chlorbutanol(3.64)   Benzoylecgonine(3.6)

ing hydrophobic moieties, as in the case of the well-known blockers Astemizole, MK-499, and Cisapride (Table 3). On the other hand, molecules characterized by lower size dimension, higher globularity, and lack of hydrophobic moieties (i.e., 4-aminopyridine, chlorbutanol, and benzoylecgonine, see Table 3) show low affinity for the hERG K^+ channel.

3.2. Prediction task

The hERG K^+ channel blocking potency of a *blind set*, disjoined from the whole *dataset* initially considered, was then estimated in a prediction work. The experimental $\log IC_{50}$ for the nine molecules composing the *blind set*, were taken from the literature.[9,32]

The mean value of predicted $\log IC_{50}$ for each molecule of the *blind set* was obtained from the two validated CO-

DESSA models. Calculated $\log IC_{50}$ values and absolute errors (E) referred to the prediction work are reported in Table 4. Statistical parameters were calculated to ascertain the correctness and the accuracy of the prediction performance, and resulted to be: $R^2 = 0.82$, $R_0^2 = 0.82$, $k = 0.94$, $(R^2 - R_0^2)/R^2 = 0$, and the mean absolute error $\bar{E} = 0.41$.

4. Conclusions

An in silico approach for predicting hERG K^+ channel blockade is proposed in this work. The study presented here allows filtering out potential hERG blockers, so giving a relevant contribution in rationalizing the development of new drugs. It ensures that undesirable leads can be identified and removed at early stages of their development, thus preventing waste of resources.

This study highlights the importance of following highly rigorous validation criteria. The application field encloses a quite large dataset, which contains different classes of drugs. As a consequence, the high molecular diversity ensures that a wide chemical space be explored in the QSAR analysis step. Moreover, the QSAR models based on CODESSA were further validated by predicting the property of interest for molecules belonging to a *blind set* (disjoined from the whole initial dataset) in order to better estimate their predictive power with regard to the chemical space where the models may be valid.

Table 4. CODESSA predicted $\log IC_{50}$ values for the *blind set*

Molecule	Experimental	CODESSA	E
Clozapine	−0.49	−0.80	−0.31
Desipramine	0.14	0.43	0.29
Mesoridazine	−0.49	−0.17	0.32
Olanzepine	−0.64	−0.42	0.22
Meperidine	1.88	2.28	0.40
Fentanyl	0.26	−0.66	−0.92
Buprenorphine	0.88	0.33	−0.55
Codeine	2.48	2.13	−0.35
Levomethadyl	0.48	0.84	0.36

The robustness and predictive ability of the models presented here were ensured by considering, for the validation step, a number of statistical parameters higher than usual. It was due to the observation, made by other authors, that a high q^2 value does not necessarily imply high predictive ability of a QSAR model; it discredits the general belief that a high value of q^2 is often considered as a proof of the high predictive power of a QSAR model.[27–30]

Several computational models have been reported recently for predicting the blocking activity of hERG channels. Most of them were derived from ligand-based approaches applied on experimental datasets containing molecules belonging to homogeneous therapeutic classes. Ekins et al. described a pharmacophoric model used to predict IC_{50} values of hERG inhibition for a test set of molecules mostly acting as antipsychotics.[6,7] Similarly, Cavalli et al. constructed a pharmacophore based on a training set of 31 QT-prolonging drugs, by means of the CoMFA approach; its predictive ability was then tested on six compounds.[8] Pearlstein et al. reported a CoMSiA model for molecules of a quite similar structure (mostly sertindole analogs).[5] Keseru developed traditional and hologram QSAR (HQSAR) models validated on three different test sets including compounds with published patch–clamp IC_{50} data and two subsets from the World Drug Index. These models revealed to possess a good predictive power in both IC_{50} and discrimination studies.[9] Pearlstein et al. published a VolSurf-based model obtained by using the IC_{50} data coming from the literature and a pharmaceutical company.[33] The IC_{50} values of inhibition were obtained for the hERG K^+ channel expressed in mammalian cells (HEK, CHO, COS, and neuroblastoma cells). PLS discriminant analysis was used to build a qualitative model. Cianchetta et al. recently supplied a relevant contribution to the studies of hERG channel blockade, by presenting computational models generated from correlation analyses of a large dataset and pharmacophore-based GRIND descriptors.[34] Finally, Rajamani et al. presented a multiple state representation of the hERG K^+ channel, which was used to construct a good prediction binding affinity model for a set of known hERG channel binders.[35]

The models described here are characterized by q^2 and R^2 values comparable to the ones obtained by the authors mentioned above. The work was carried out on a quite large dataset characterized by IC_{50} values of inhibition of the hERG channel only expressed in mammalian HEK cells. Furthermore, in order to accurately validate these QSAR models, a number of conditions higher than usual were taken into account. In particular, R_0^2, k, and the ratio $(R^2 - R_0^2)/R^2$ were calculated, they resulted to be in agreement with the imposed criteria described in Section 2.4. The selected models also show good accuracy in predicting the IC_{50} values of a further *blind set* considered for validation. Eight of the nine molecules were correctly identified as *blocking* or *not-blocking* agents.

Therefore, the in silico approach presented here could be considered as a valuable tool for practical applications in predicting the blockade of hERG K^+ channels.

References and notes

1. Calderone, V.; Cavero, I. *Minerva Med.* **2002**, *93*, 181.
2. Vandenberg, J. I.; Walzer, B. D.; Campbell, T. *Trends Pharmacol. Sci.* **2001**, *22*, 240.
3. Aronov, A. M. *Drug Discov. Today* **2005**, *10*, 149, Review.
4. Mitcheson, J. S.; Chen, J.; Lin, M.; Culberson, C.; Sanguinetti, M. C. *Proc. Natl. Acad. Sci. U.S.A.* **2000**, *97*, 12329.
5. Pearlstein, R. A.; Vaz, R. J.; Kang, J.; Chen, X.-L.; Preobrazhenskaya, M.; Shchekotikhin, A. E.; Korolev, A. M.; Lysenkova, L. N.; Miroshnikova, O. V.; Hendrix, J.; Rampea, D. *Bioorg. Med. Chem. Lett.* **2003**, *13*, 1829.
6. Ekins, S.; Crumb, W. J.; Sarazan, R. D.; Wikel, J. H.; Wrighton, S. A. *J. Pharmacol. Exp. Ther.* **2002**, *301*, 427.
7. Ekins, S. *Biochem. Soc. Trans.* **2003**, *31*, 611.
8. Cavalli, A.; Poluzzi, E.; De Ponti, F.; Recanatini, M. *J. Med. Chem.* **2002**, *45*, 3844.
9. Keseru, G. M. *Bioorg. Med. Chem. Lett.* **2003**, *13*, 2773.
10. Curran, M. E.; Splawski, I.; Timothy, K. W.; Vincent, G. M.; Green, E. D.; Keating, M. T. *Cell* **1995**, *80*, 795.
11. Katritzky, A. R.; Lobanov, V. S.; Karelson, M., *CODESSA: Reference Manual*; *Version 2;* University of Florida, 1994.
12. Bains, W.; Basman, A.; White, C. *Prog. Biophys. Mol. Biol.* **2004**, *86*, 205, Review.
13. Ridley, J. M.; Milnes, J. T.; Zhang, Y. H.; Witchel, H. J.; Hancox, J. C. *J. Physiol.* **2003**, *549*, 667.
14. Kiehn, J.; Thomas, D.; Karle, C. A.; Schols, W.; Kubler, W. *Naunyn-Schmiedeberg's Arch. Pharmacol.* **1999**, *359*, 212.
15. Scholz, E. P.; Zitron, E.; Kiesecker, C.; Lueck, S.; Kathoefer, S.; Thomas, D.; Weretka, S.; Peth, S.; Kreye Volker, A. W.; Schoels, W.; Katus, H. A.; Kiehn, J.; Karle, C. A. *Naunyn-Schmiedeberg's Arch. Pharmacol.* **2003**, *368*, 404.
16. Danielsson, B. R.; Lansdell, K.; Patmore, L.; Tomson, T. *Epilepsy Res.* **2003**, *55*, 147.
17. Kornick, C. A.; Kilborn, M. J.; Santiago-Palma, J.; Schulman, G.; Thaler, H. T.; Keefe, D. L.; Katchman, A. N.; Pezzullo, J. C.; Ebert, S. N.; Woosley, R. L.; Payne, R.; Manfredi, P. L. *Pain* **2003**, *105*, 499.
18. Stanat, S. J. C.; Carlton, C. G.; Crumb, W. J.; Agrawal, K. C.; Clarkson, C. W. *Mol. Cell. Biochem.* **2003**, *254*, 1.
19. Hu, S.; Wang, S.; Gibson, J.; Gilbertson, T. A. *J. Pharmacol. Exp. Ther.* **1998**, *287*, 480.
20. Shimizu, A.; Niwa, R.; Lu, Z.; Honjo, H.; Kamiya, K. *Environ. Med.* **2003**, *47*, 48.
21. Milnes, J. T.; Crociani, O.; Arcangeli, A.; Hancox, J. C.; Witchel, H. J. *Br. J. Pharmacol.* **2003**, *139*, 887.
22. Kushida, S.; Ogura, T.; Komuro, I.; Nakaya, H. *Eur. J. Pharmacol.* **2002**, *457*, 19.
23. Wu, L.-M.; Orikabe, M.; Hirano, Y.; Kawano, S.; Hiraoka, M. *J. Cardiovasc. Pharmacol.* **2003**, *42*, 410.
24. Crumb, W. J. Jr, Personal comunication, 9 August 2000.
25. SYBYL, Version 7, TRIPOS Assoc., St. Louis, MO., http://www.tripos.com.

26. Testai, L.; Bianucci, A. M.; Massarelli, I.; Breschi, M. C.; Martinotti, E.; Calderone, V. *Curr. Med. Chem.* **2004**, *11*, 763.
27. Novellino, E.; Fattorusso, C.; Greco, G. *Pharm. Acta Helv.* **1995**, *70*, 149.
28. Norinder, U. *J. Chemomet.* **1996**, *10*, 95.
29. Kubinyi, H.; Hamprecht, F. A.; Mietzner, T. *J. Med. Chem.* **1998**, *41*, 2553.
30. Golbraikh, A.; Tropsha, A. *J. Mol. Graphics Modell.* **2002**, *20*, 269.
31. Karelson, M. *Molecular Descriptors in QSAR/QSPR*; Wiley: New York, 2000.
32. Katchman, A. N.; Mc Groary, K. A.; Kilborn, M. J.; Kornick, C. A.; Manfredi, P. L.; Woosley, R. L.; Ebert, S. N. *J. Pharmacol. Exp. Ther.* **2002**, *303*, 688.
33. Pearlstein, R.; Vaz, R.; Rampe, D. *J. Med. Chem.* **2003**, *46*, 2017.
34. Cianchetta, G.; Li, Y.; Kang, J.; Rampe, D.; Fravolini, A.; Cruciani, G.; Vaza, R. J. *Bioorg. Med. Chem. Lett.* **2005**, *15*, 3637.
35. Rajamani, R.; Tounge, B. A.; Li, J.; Reynolds, C. H. *Bioorg. Med. Chem. Lett.* **2005**, *15*, 1737.